Well-Defined Diblock Copolymers Possessing Fluorescent and Metal Chelating Functionalities as Novel Macromolecular Sensors for Amines and Metal Ions

Maria Demetriou, Theodora Krasia-Christoforou

Department of Mechanical and Manufacturing Engineering, University of Cyprus, P.O. Box 20537, 1678 Nicosia, Cyprus
Correspondence to: T. Krasia-Christoforou (E-mail: krasia@ucy.ac.cy)

Received 6 May 2011; accepted 25 August 2011; published online 15 September 2011
DOI: 10.1002/pola.24977

ABSTRACT: The amino- and metal-ion sensing capability of a novel type of well-defined block copolymers based on 9-anthrylmethyl methacrylate (AnMMA; hydrophobic, fluorescent) and 2-(acetoacetoxy)ethyl methacrylate (AEMA; hydrophobic, metal chelating) has been investigated in organic media. AEMA$_x$-*b*-AnMMA$_y$ diblock copolymers were prepared for the first time using reversible addition-fragmentation chain transfer (RAFT) polymerization. All polymers were characterized in terms of molecular weights, polydispersity indices and compositions by size exclusion chromatography and ^{1}H NMR spectroscopy, respectively. The glass transition (T_g) temperatures of the AEMA$_x$ and AnMMA$_x$ homopolymers and the AEMA$_x$-*b*-AnMMA$_y$ diblock copolymers were determined using differential scanning calorimetry. These systems were evaluated toward their ability to act as effective dual chemosensors (i.e., amino- and metal-ion sensors) in an organic solvent (chloroform). More precisely, the fluorescence intensity of both the AnMMA$_x$ homopolymers and the AnMMA$_x$-*b*-AEMA$_y$ diblock copolymers in solution exhibited a significant decrease in the presence of triethylamine. Moreover, the presence of iron (III) cations were also found to significantly affect the fluorescence signal of the anthracene moieties when those were combined in a block copolymer structure with the AEMA units, due to complex formation occurring between the β-ketoester groups of the AEMA$_x$ segment and the cations. © 2011 Wiley Periodicals, Inc. J Polym Sci Part A: Polym Chem 50: 52–60, 2012

KEYWORDS: block copolymers; fluorescence; reversible addition-fragmentation chain transfer (RAFT)

INTRODUCTION Polymeric materials possessing fluorescent moieties have attracted significant attention because of their potential applications such as fluorescent chemosensors[1,2] and biosensors,[3] fluorescent imaging agents,[4,5] optical materials for organic light emitting devices,[6] and metal-ion sensors,[7] to mention only a few.

A widely used fluorescent molecule known for its interesting photophysical properties is anthracene, a polycyclic aromatic hydrocarbon.[8–10] Because of the lack of interaction with polymeric materials, the anthracene group has been selected by various research teams to be introduced into polymers.[11] Anthracene-containing polymers have been used in the fabrication of optoelectronic devices,[12–14] photoluminescent films,[15,16] photoresists,[17,18] chemiluminescent fluorophores,[19–21] and so forth.

To date, a limited number of reports appear in the literature, dealing with the preparation of well-defined polymers based on 9-anthrylmethyl methacrylate (AnMMA). Instead, most reports refer to the noncontrollable conventional free radical polymerization of anthracene-containing monomers.[17,18] An established controlled radical polymerization process namely atom transfer radical polymerization, although successfully used in the preparation of well-defined polymers based on anthracene,[22,23] fails in preparing well-defined polymers based on 2-(acetoacetoxy)ethyl methacrylate (AEMA), the second monomer used in this study.[24]

Fluorescence quenching is an effective mechanism that can be used for the identification of ions (both cations and anions) in solution.[25,26] A structural requirement of a fluorescent metal-ion sensor is the coexistence of a light-emitting and a metal receptor group linked together via covalent bonding. For high sensor efficiency, the ion–receptor interaction must be able to modify the fluorescence properties of the light-emitting group.[27,28] Numerous examples appear in the literature describing the chemosensing ability of small molecules combining a fluorescent group with a metal binding moiety.[29–31] Currently, the design and synthesis of polymer-based metal ion sensors combining fluorescent and metal-chelating groups presents high interest. Polymer-based metal-ion sensors have been reported by various groups.[32–35] However, most of the developed systems are homopolymers characterized by a structural complexity and

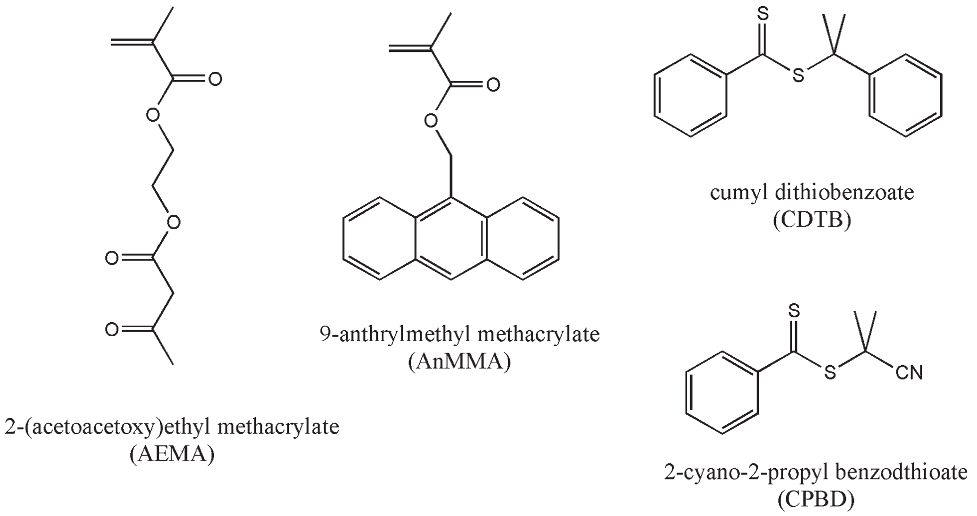

FIGURE 1 Chemical structures of the two monomers and the CTAs used in this study.

demanding synthetic methodologies toward their preparation. In this work, a simple and cost-effective synthetic approach involving a controlled radical polymerization process was used toward this purpose.

We have chosen to combine AnMMA with AEMA, a monomer possessing bidentate β-dicarbonyl moieties in a diblock copolymer architecture. The well-known strong affinity of the latter to multivalent cations[36] prompted some groups to synthesize polymers with β-dicarbonyl or β-ketoester repeating units.[37–41] We first used two different routes for the preparation of well-defined coordinating block copolymers bearing β-ketoester functionalities involving group transfer polymerization[42] and reversible addition-fragmentation chain transfer (RAFT) polymerization.[24] RAFT represents a versatile polymerization technique that allows for the preparation of well-defined polymers of various architectures,[43] such as block copolymers,[44–48] star polymers,[49–51] graft polymers,[52] hyperbranched polymers,[53–56] and polymer (co)networks.[57–59] The process shows many of the characteristics of "living" polymerizations, that is, control over the molecular weight (MW), narrow MW distributions (MWDs) and linear MW-conversion profiles.[60] Furthermore, RAFT is compatible with a wide range of monomers[61] and reaction conditions.[62,63] For the first time, AEMA is combined with AnMMA to yield well-defined functional diblock copolymers presenting fluorescent and metal chelating properties. Hence, this work describes the unique combination of a rare example of a ligating monomer polymerized by RAFT, with a fluorescent polymethacrylate, the controlled polymerization of which has been rarely reported. The RAFT process was readily used to prepare well-defined AnMMA$_x$ homopolymers as well as diblock copolymers based on AnMMA and AEMA. The molecular and compositional characteristics of the resulting homopolymers and copolymers were determined by size exclusion chromatography (SEC) and ^{1}H NMR spectroscopy, respectively. Furthermore, differential scanning calorimetry (DSC) was used for determining the glass tranasition temperature(s) of the polymers.

This is the first demonstration of the capability of well-defined block copolymer systems possessing specific functionalities within the two block segments (i.e., fluorescent and metal binding) to act as effective dual-chemosensors for (i) compounds with lone electron pairs such as amines and (ii) transition metal ions. The latter, that is, the effectiveness of the AEMA$_x$-*b*-AnMMA$_y$ diblock copolymers toward metal-ion sensing is demonstrated by the strong fluorescence quenching observed on complexation of the ions with the strong bidentate β-ketoester groups present on the AEMA$_x$ chelating block segment.

RESULTS AND DISCUSSION

Figure 1 illustrates the chemical structures and names of monomers, initiator and the chain transfer agents (CTA) used for polymer synthesis.

Molecular Weights and Composition of the AEMA$_x$ and AnMMA$_x$ Homopolymers and the AEMA$_x$-*b*-AnMMA$_y$ Diblock Copolymers

Well-defined AEMA$_x$ and AnMMA$_x$ homopolymers and AEMA$_x$-*b*-AnMMA$_y$ diblock copolymers were successfully synthesized following typical RAFT methodologies described in Experimental section. The RAFT polymerization of the AEMA monomer first described by Krasia et al.[24] proceeds in a well-controlled manner resulting in polymers characterized by monomodal and narrow MWDs. To the best of our knowledge for the first time in this study, well-defined AnMMA$_x$ homopolymers and AEMA$_x$-*b*-AnMMA$_y$ diblock copolymers are prepared by RAFT. The molecular characterization of these materials was carried out by means of SEC and ^{1}H NMR. Table 1 summarizes the chemical structures of all homopolymers and diblock copolymers prepared in this study along with their MW and composition characteristics.

Low to moderate polydispersity indices (PDIs) were observed for the homopolymers and diblock copolymers, varying between 1.23 and 1.43. However, as seen in the table low polymerization yields were obtained in the cases of the

TABLE 1 Characteristics of the Homopolymers and Block Copolymers Based on AEMA and AnMMA Obtained by RAFT (Polymerization Yields, Molecular Weights, and Polydispersity Indices)

			SEC Results[c]	
Experimental Structure[a]	Yield (%)	Theor. MW[b] (g mol^{-1})	M_n	PDI
AnMMA$_{36}$ (CDTB)	37.5	18,381	16,177	1.31
AnMMA$_{47}$ (CPBD)	90	25,062	13,228	1.27
AEMA$_{42}$ (CDTB)	85	5,694	9,235	1.23
AEMA$_{42}$-*b*-AnMMA$_{83}$ (CDTB)	17	17,688	18,802	1.33
AEMA$_{42}$-*b*-AnMMA$_{113}$ (CDTB)	20	25,810	38,870	1.43
AEMA$_{21}$ (CDTB)	90	2,414	4,749	1.26
AEMA$_{21}$-*b*-AnMMA$_{43}$ (CDTB)	25	14,279	15,822	1.34

[a] Determined by SEC and ^{1}H NMR.

[b] [(g monomer)/(mol RAFT agent)] × (polymerization yield) + MW of CTA (for homopolymers) and [(g monomer)/(mol CTA agent)] × (polymerization yield) + M_n of macro-CTA (for diblock copolymers).

[c] M_n: number average molecular weight; PDI: polydispersity index; CDTB: cumyl dithiobenzoate; CPBD: 2-cyano-2-propylbenzodithioate.

AnMMA$_x$ homopolymer and the AEMA$_x$-*b*-AnMMA$_y$ diblock copolymers when cumyl dithiobenzoate (CDTB) was used as the CTA. A significant increase in the polymerization yield was observed when 2-cyano-2-propylbenzodithioate (CPBD) was used instead as the CTA for the preparation of the AnMMA$_x$ homopolymer by following exactly the same experimental conditions. As reported by Moad et al.,[61] at certain RAFT agent concentrations, retardation—that is partially manifested by an inhibition period corresponding to the required time to convert the RAFT agent into a polymeric RAFT agent—occurs in a much less extent in the case of CPBD compared to CDTB.

Figure 2 displays the SEC traces of the AEMA$_{21}$ homopolymer and the corresponding AEMA$_{21}$-*b*-AnMMA$_{43}$ diblock copolymer. The MWD of the latter is shifted toward higher MWs compared to that of the homopolymer, demonstrating the block efficiency from homopolymer to block copolymer.

The expected chemical structure of the polymers was confirmed by ^{1}H NMR spectroscopy. Figure 3 shows the ^{1}H NMR spectra of the AEMA$_{21}$ homopolymer and the AEMA$_{21}$-*b*-AnMMA$_{43}$ diblock copolymer.

The peak assignments are shown in the spectra. The AEMA comonomer compositions were determined from the ratio of the areas under the characteristic signals of the AEMA and AnMMA, appearing at 3.6 and 5.6 ppm, respectively.

Thermal Properties

DSC measurements provided the glass transition (T_g) temperatures of the AEMA$_x$ and AnMMA$_x$ homopolymers and the

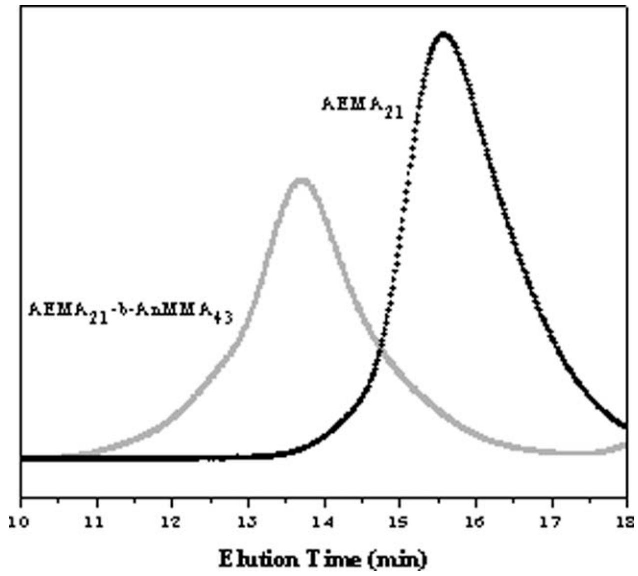

FIGURE 2 SEC eluograms of the AEMA$_{21}$ (black) and the AEMA$_{21}$-*b*-AnMMA$_{43}$ (gray).

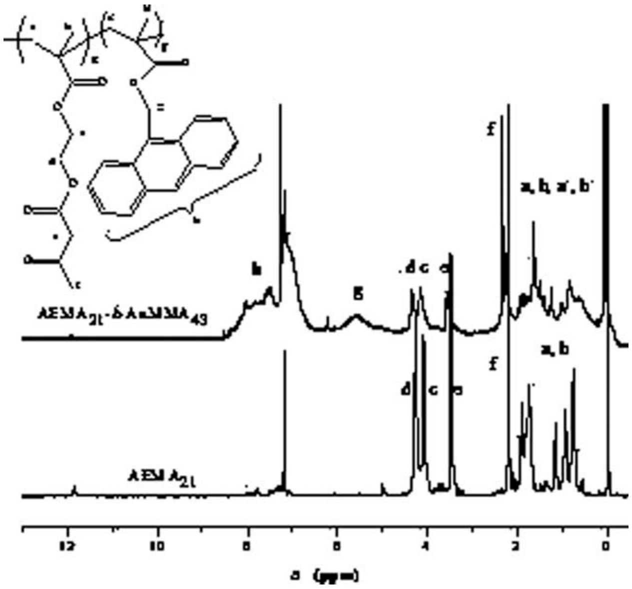

FIGURE 3 ^{1}H NMR spectra of the AEMA$_{21}$ homopolymer and the AEMA$_{21}$-*b*-AnMMA$_{43}$ diblock copolymer.

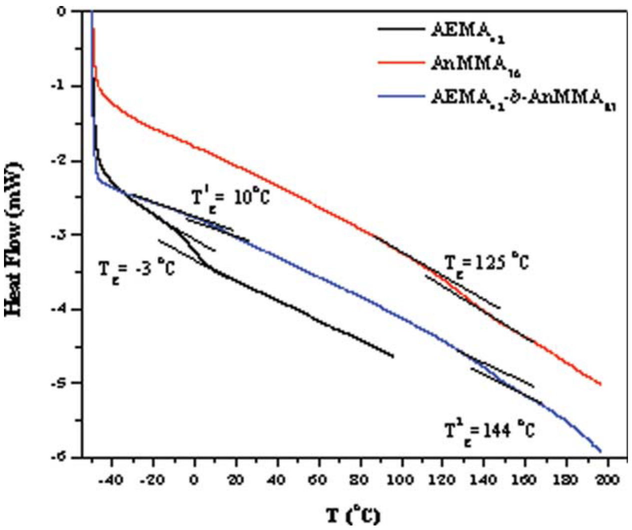

FIGURE 4 DSC thermograms of the AEMA$_{42}$ homopolymer, the AnMMA$_{36}$ homopolymer, and the AEMA$_{42}$-*b*-AnMMA$_{83}$ diblock copolymer.

AEMA$_x$-*b*-AnMMA$_y$ diblock copolymers. The T_g of the AEMA$_x$ homopolymer was determined to be -3 °C, which is close to our previous findings[24] whereas the T_g of the AnMMA$_x$ homopolymer was found to be around 125 °C. Block copolymers exhibited two T_gs ($\sim$10 °C for the AEMA$_x$ block and $\sim$144 °C for the AnMMA$_y$ block), suggesting that microphase separation may exist in the bulk. In general, the T_gs in block copolymers can be influenced by the sizes of the phases generated and the compatibility of the different components (blocks). According to Buzin et al.[64] in the case where the two blocks in a diblock copolymer are incompatible, the lengths of the two segments are the determining factor for the sizes of the phases generated due to microphase separation; the morphology of the latter will depend on their ratio. The T_gs of both components are affected by the continuing molecules that cross the interface. Depending on the phase mobility, variation in the T_gs of the different block segments can be observed compared to the T_g values of the corresponding homopolymers. Moreover, in the case of the AnMMA segment, the observed differences in the glass transition of the AnMMA$_{36}$ homopolymer and the AnMMA$_{83}$ block segment incorporated within the diblock copolymer (appearing at 125 and 144 °C, respectively) may be reinforced by the increased MW and the more pronounced π–π interactions occurring between the AnMMA aromatic side chains of the AnMMA$_{83}$ segment present in the diblock, which promotes chain immobility.[65]

Fluorescence Sensing Toward Amines

Electron donating groups located in the proximity of anthracene moieties result in a drastic decrease in the fluorescence intensity of anthracene due to electron transfer phenomena occurring between the lone electron pair of the amines and the photoexcited anthracene units.[66]

The AnMMA$_{36}$ and AEMA$_{42}$-*b*-AnMMA$_{83}$ systems were examined toward their ability to act as macromolecular sensors for amines in organic solvents. To demonstrate the effectiveness of these new polymers toward amine sensing, triethylamine was chosen as an example. For this purpose, the fluorescence intensity of a polymer solution was monitored in the presence of various concentrations of triethylamine (ranging from 3.6 mM to 1 M). As seen in Figure 5, an increase in the amount of the amine present in solution causes a decrease in the fluorescence intensity. As previously stated, the fluorescence quenching through electron transfer requires that the amine is adjacent to the anthryl groups.[66] The presence of triethylamine at a much higher concentration (varying between 3.6 mM and 1 M) compared to the concentration of the anthracene moieties within the copolymer (1×10^{-4} M) renders the electron transfer process possible.

It should be noted at this point that the possibility of electron transfer from the anthracene groups to chloroform molecules is not possible;[11] hence, the fluorescence quenching is sorely attributed to the electron transfer of the electron lone pair of triethylamine to the anthracene moieties as illustrated in Figure 5.

Fluorescence Sensing Toward Metal Ions

The AEMA$_x$-*b*-AnMMA$_y$ block copolymers are expected to complex and solubilize different metal-ion salts in organic media due to the presence of the strong bidentate β-ketoester groups within their structure. The latter are known to act as effective stabilizers for various metal ions of different geometries and oxidation states.[36]

The β-ketoester moiety exists in two tautomeric forms (the keto and the enol) which are in equilibrium. Both tautomers are capable of complexing transition metal ions. For the systems investigated in this study (AEMA$_x$-*b*-AnMMA$_y$), the ^{1}H NMR spectra recorded in $CDCl_3$ (an example is presented in Fig. 3) show that the keto tautomer is the dominant one.

The ability of the AEMA$_x$-*b*-AnMMA$_y$ diblock copolymers toward metal-ion sensing (Fe(III)) has been investigated in chloroform. Chloroform is a common solvent for both blocks in these copolymer systems; hence, the polymer exists only as unimers in solution. On $FeCl_3 \cdot H_2O$ addition in the solution, a color change was observed within a few seconds from light yellow to deep wine red, attributed to the complex formation between the Fe(III) ion and the β-ketoester groups. Presumably, as shown in Figure 6, the octahedral structure of the ferric salt is preserved and only the four water molecules adjacent to the iron atoms are replaced by two keto tautomeric β-ketoester ligands. Figure 7 presents the ultra-violet/visible (UV–Vis) spectrum of the AEMA$_{42}$-*b*-AnMMA$_{83}$/$FeCl_3 \cdot 6H_2O$ complex in chloroform. In the spectrum, the signal appearing at 550 nm confirms the complex formation.[67]

As chloroform is a good solvent for the $FeCl_3 \cdot 6H_2O$ salt, it should be mentioned that an excess of chloroform favors decomplexation. This is indicated by a color change of the solution on dilution, from wine red to yellow/orange (color of $FeCl_3 \cdot 6H_2O$ in $CHCl_3$).

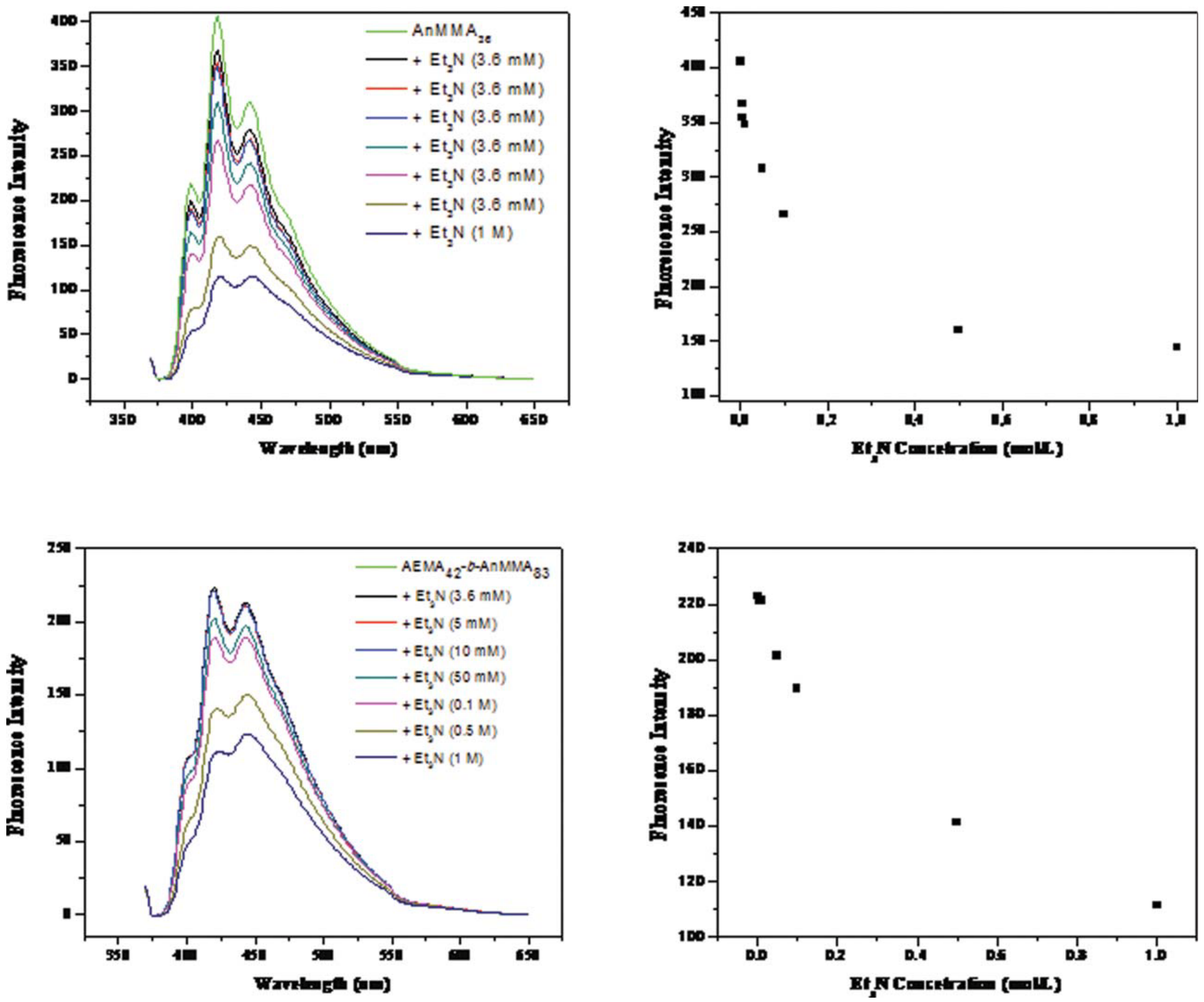

FIGURE 5 AnMMA$_{36}$ and AEMA$_{42}$-*b*-AnMMA$_{83}$ fluorescence spectra (polymer concentration $= 10^{-4}$ M based on anthracene groups) recorded in chloroform in the presence of different quencher (Et$_3$N) concentrations, ranging from 3.6 mM to 1 M.

It is noteworthy to emphasize at this point the importance of the use of a block copolymer structure toward Fe(III) sensing in this particular solvent, since, as previously demonstrated,[67] complexation of $FeCl_3 \cdot 6H_2O$ performed in chloroform using poly(butyl methacrylate)-*block*-poly((2-acetoacetoxy)ethyl methacrylate) (BuMA$_x$-*b*-AEMA$_y$) revealed that the coordination of the Fe(III) onto the AEMA$_y$ segment reduced its solubility in that particular solvent. The latter resulted in the formation of aggregates consisting of a poly (AEMA)-metal ion core and a poly(BuMA) corona. Therefore, it is expected that in the case of a random copolymer consisting of AnMMA and AEMA units, the complexation of Fe(III) ions with the latter will cause the destabilization of the random copolymer chains in solution due to the fact that these are not capable of self-organizing into soluble core-shell micellar nanostructures.

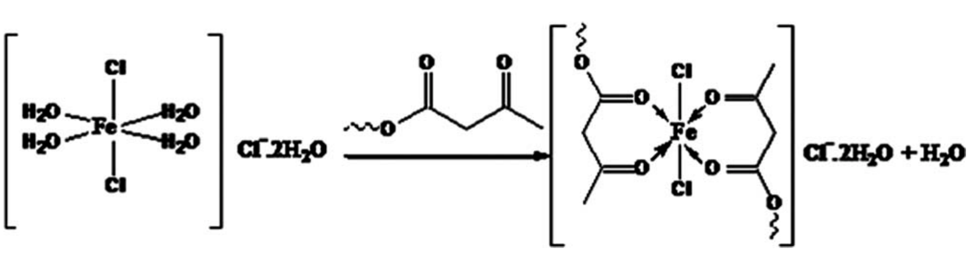

FIGURE 6 Substitution of "L" type of ligand molecules (H_2O) in $FeCl_3 \cdot 6H_2O$ by the "keto" form of the β-ketoester group.

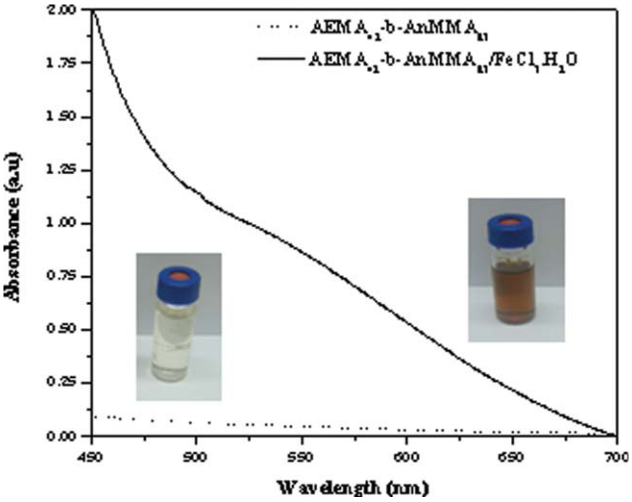

FIGURE 7 UV–Vis spectrum of AEMA$_{42}$-*b*-AnMMA$_{83}$/FeCl$_3$·6H$_2$O complex formed by the keto form of the β-ketoester ligands in chloroform.

Based on the above, it is expected that in the case of the AEMA$_x$-*b*-AnMMA$_y$/Fe(III) systems, micellar nanostructures are generated in solution, consisting of a poly(AEMA)-Fe(III) core. It is assumed that this self-organized micellar nanoenvironment leads to the confinement of the complexed transition metal ion and of the fluorescent moieties within nanosized domains, reinforcing the interaction between the two, thus promoting chelation-enhanced fluorescence quenching.

Figure 8 presents the fluorescence quenching curves recorded in chloroform at 368 nm excitation wavelength (λ_{exc}) as a function of the concentration of the Fe(III) salt. As seen in the graphs, a drastic decrease in the fluorescence intensity is observed on complexation. As expected, the quenching effect on the anthracene chromophore is further enhanced on increasing the salt concentration in the system. These results are in agreement with similar observations reported by other groups[7] and have been attributed to the presence of unpaired d electrons in transition metal ions that can effectively quench the anthryl chromophore. According to Buruiana et al.,[11] the quenching processes that can take place in anthracene-containing systems may involve different quenching mechanisms namely excimer or exciplex formation, metal–π complex, electron transfer and energy transfer. Paramagnetic metal ions such as Fe(III) (d^5) possessing unpaired d electrons, when present at high concentrations lead to an effective quenching of the anthracene fluorescence. The possible quenching mechanism in the AEMA$_x$-b-AnMMA$_y$/Fe(III) systems may involve the energy transfer from the singlet excited-state anthracene chromophores to the low-lying half-filled 3d orbitals of the Fe(III) paramagnetic cation.[68] Moreover, the decrease in the fluorescence intensity is accompanied by a blue shifting in the spectrum. Blue shifts in the fluorescence spectra were previously observed on complexation of Fe^{3+} as well as other metal ions including Pb^{2+}, Fe^{2+}, Cu^{+}, Sb^{3+} and lanthanides with polymers.[28,69]

EXPERIMENTAL

Materials and Methods

Benzene (Fluka, ≥ 99.5%), ethyl acetate (Scharlau, 99%), tetrahydrofuran (Scharlau, 99.9%) were stored over CaH$_2$ (Merck, 99.9%) and distilled under reduced pressure immediately prior to the polymerization reactions. Chloroform (Scharlau, 99.9%) was dried over anhydrous MgSO$_4$. Methanol (LabScan, 99.9%), *n*-hexane (LabScan, 99%), toluene (Sigma-Aldrich), HCl (Merck, 37% solution), diethyl ether (LabScan, 99.5%), benzoic acid (Merck, 99%), aqueous solution of tetrabutylammonium hydroxide (Sigma-Aldrich, 40% wt), triethylamine (Merck, ≥99%), pyridine (Sigma-Aldrich, ≥99.9% [HPLC]), benzyl chloride (Sigma-Aldrich, 99%), carbon tetrachloride (Riedel de Haën, ≥99.8%), α-methylstyrene (Sigma-Aldrich, 99%), sodium methoxide (Aldrich, 30% solution in methanol), methacryloyl chloride (Sigma-Aldrich), 9-anthracenemethanol (Aldrich, 97%), 2-cyano-2-propyl benzodithioate (Sigma-Aldrich, >97% [HPLC]) and deuterated chloroform (Merck) were used as received by the manufacturer. The following inorganic compounds were used without further purification: Sulfur (Aldrich, powder ~100 mesh), silica gel (Aldrich, 60 Å, 70–230 mesh), NaOH pellets (Scharlau), NaHCO$_3$ (Sigma-Aldrich, 99.5%), NaCl (HiMedia), and anhydrous MgSO$_4$ (Scharlau). 2-Acetoacetoxy ethyl methacrylate (Aldrich, 95%) was passed through a basic alumina column prior to the polymerizations and used without further purification. 2,2-Azobis(isobutylnitrile) (AIBN, Sigma-Aldrich, 95%) was recrystallized twice from ethanol and dried *in vacuo* at room temperature for 3 days.

Synthesis of Cumyl Dithiobenzoate (chain transfer agent)

CDTB was synthesized in two steps, following a procedure reported by Rizzardo and coworkers.[70] Briefly, the first step involved the preparation of dithiobenzoic acid via the reaction of sulfur, sodium methoxide, and benzyl chloride in

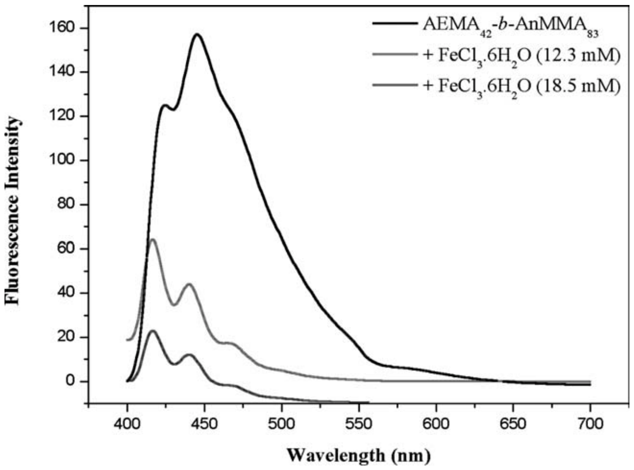

FIGURE 8 AEMA$_{42}$-*b*-AnMMA$_{83}$ (polymer concentration = 10^{-4} M based on anthracene groups) fluorescence spectra recorded in chloroform in the presence of different quencher (FeCl$_3$·6H$_2$O) concentrations (12.3 and 18.5 mM).

methanol at room temperature for 18 h. Subsequently, dithiobenzoic acid was left to react with α-methylstyrene in carbon tetrachloride at 70 °C for 18 h to obtain CDTB in 19.3% yield after purification by column chromatography (silica gel), using *n*-hexane as a solvent.

^{1}H NMR (300 MHz, CDCl$_3$) δ (ppm): 7.87 (d, 2H), 7.58–7.22 (m, 8H), 2.01 (s, —CH$_3$).

Synthesis of 9-Anthrylmethyl Methacrylate, AnMMA

For the synthesis of the AnMMA, anthracenemethanol (3 g, 0.014 mol) was dissolved in tetrahydrofuran (12 mL). Subsequently, triethylamine (3 mL, 0.016 mol), pyridine (2 mL, 0.016 mol), and methacryloyl chloride (2.1 mL, 0.016 mol) were added with a 20% excess, in the reaction flask. The methacryloyl chloride was added dropwise during stirring at 0 °C. After addition, the mixture was allowed to reach room temperature and was then left to stir for 1 h. Continuously, water (10 mL) was added and the mixture was extracted with diethyl ether followed by the extraction of the organic phase with HCl (1 M, 3× 5 mL), then with NaHCO$_3$ solution (5% in water 3× 5 mL) and with a saturated NaCl solution (3× 5 mL). Afterward, the solvent was removed under reduced pressure and the product was recrystallized from methanol (42% yield).

^{1}H NMR (300 MHz, CDCl$_3$) δ (ppm): 7.2–8.5 (m, —Ph), 6.2 (s, —CH$_2$Ph), 6.05 (s, —Ph), 5.50 (s, —Ph), 5.30 (s, =CH$_2$), 3.49 (s, =CH$_2$), 2.17 (s, —CH$_2$), 1.9 (—CH$_3$).

Synthesis of AnMMA Homopolymers

AnMMA (800 mg, 2.87 mmol) was placed in a round-bottom flask and dissolved in freshly distilled benzene (1.2 mL) under a dry nitrogen atmosphere. CDTB (7.89 mg, 0.029 mmol) and AIBN (2.61 mg, 0.016 mmol) were dissolved in benzene and then were transferred into the flask via a syringe. The reaction mixture was degassed by three freeze–evacuate–thaw cycles, and placed under a dry nitrogen atmosphere at 65 °C for 20 h. The polymerization was terminated by cooling the reaction down to room temperature. The produced homopolymer (300 mg, 37.5% polymerization yield) was retrieved by multiple precipitations in methanol and was left to dry *in vacuo* at room temperature for 24 h. The synthesis of AnMMA$_x$ was also carried out using the commercially available CPBD (6.4 mg, 0.029 mmol) as the CTA following the same experimental conditions (718.7 mg, 89.8% polymerization yield).

^{1}H NMR (300 MHz, CDCl$_3$) δ (ppm): 7.2–8.5 (m, br, Ph), 6.2 (br, —CH$_2$Ph), 1.99–0.7 (—CH$_2$, —CH$_3$).

Synthesis of AEMA Homopolymers

To a round-bottom flask (25 mL) maintained under a dry nitrogen atmosphere, AEMA (2.7 mL, 14.0 mmol) was added. CDTB (127 mg, 0.47 mmol) and AIBN (14.0 mg, 0.09 mmol) were dissolved in freshly distilled ethyl acetate (3.0 mL) and were transferred into the flask with the aid of a syringe. Subsequently, the resulting solution was degassed by three freeze–evacuate–thaw cycles, placed under a dry nitrogen atmosphere and heated at 65 °C for 20 h. The polymerization was terminated by cooling the reaction down to room temperature. The produced AEMA$_x$ (2.48 g, 85% polymerization yield) was retrieved by precipitation in methanol and was left to dry *in vacuo* at room temperature for 24 h.

^{1}H NMR (300 MHz, CDCl$_3$) δ (ppm): 11.90 (s, —OH (enol)), 5.10 (br, s, =CH (enol)), 4.2 (s, —CH$_2$), 4.08 (s, —CH$_2$), 3.6 (s, —CH$_2$), 1.8 (s, —COCH$_3$), 1.74–0.76 (—CH$_2$, —CH$_3$).

Synthesis of AEMA$_x$-*b*-AnMMA$_y$ Diblock copolymers

To a round-bottom flask, the macro-CTA, AEMA$_{42}$ (M_n^{SEC} = 9,235 g mol^{-1}, 200 mg, 0.022 mmol) was placed and kept under a dry nitrogen atmosphere. AIBN (1.6 mg, 0.0096 mmol) and AnMMA (1.08 g, 3.909 mmol) dissolved in tetrahydrofuran (1.3 mL) were then transferred into the flask via a syringe. The reaction mixture was degassed by three freeze–evacuate–thaw cycles and placed under a dry nitrogen atmosphere at 62 °C for 20 h. The polymerization was terminated by cooling the reaction down to room temperature. The produced diblock copolymer was retrieved by multiple precipitations in methanol and was left to dry *in vacuo* at room temperature for 24 h.

^{1}H NMR (300 MHz, CDCl$_3$) δ (ppm): 11.90 (s, —OH (enol)), 7.16–8.03 (br, —Ph), 5.6 (br, —NCH$_2$), 4.35 (s, —CH$_2$), 4.16 (s, —CH$_2$), 3.56 (s, —CH$_2$), 2.35 (s, —COCH$_3$), 0.85–1.74 (br, —CH$_2$, —CH$_3$).

Characterization

NMR spectra were recorded in CDCl$_3$ with tetramethylsilane used as an internal standard using an Avance Brucker 300 MHz spectrometer equipped with an Ultrashield magnet. The MWs and PDIs of the polymers were determined by SEC using equipment supplied by Polymer Standards Service (PSS). All measurements were carried out at room temperature using Styragel HR 3 and Styragel HR 4 columns. The mobile phase was THF, delivered at a flow rate of 1 mL min^{-1} using a Waters 515 isocratic pump. The refractive index was measured with a Waters 2414 refractive index detector supplied by PSS. The instrumentation was calibrated using poly(methyl methacrylate) standards with low PDI (MWs of 7,39,000, 4,46,000, 2,70,000, 1,26,000, 65,000, 31,000, 1,44,00, 4,200, 1,580, 670, 450, and 102 (methyl isobutyrate) g mol^{-1}) supplied by PSS. DSC was used to measure the T_gs of the homopolymers, and block copolymers using a Q100 TA Instrument with a heating rate of 10 °C min^{-1}. Each sample was scanned twice between -100 and $+150$ °C. The second run (heat) was used for data analysis. UV–Vis spectra were recorded at room temperature using dual-beam grating spectrophotometer (Jasco V-630). Measurements were carried out in chloroform by placing the solutions in a 1 cm quartz cells. Fluorescence emission spectra were recorded in chloroform by using a Jasco 6300 spectrofluorimeter. The excitation wavelength was set at 368 nm. The polymer concentration in solution was 1×10^{-4} M (polymer concentration based on anthracene groups) whereas the concentration of the triethylamine varied from 3.6 mM to 1 M and of the FeCl$_3$·6H$_2$O 12.3 and 18.5 mM.

CONCLUSIONS

In summary, we have presented for the first time the effectiveness of well-defined methacrylate-based AEMA$_x$-*b*-AnMMA$_y$ diblock copolymers possessing β-ketoester metal chelating and anthryl fluorescent side-chain functionalities to act as dual-chemosensors for amines and transition metal ions in organic solvents. The preparation of these systems involved an easy, cost-effective, and versatile controlled radical polymerization technique that enabled the synthesis of polymeric materials characterized by predetermined MWs and low MWD. The aforementioned block copolymer chemosensors and the simple strategy followed for their synthesis may be useful in the design and development of new and efficient chemosensors in the future.

This work was financially supported by the Cyprus Research Promotion Foundation (Program ΤΕΧΝΟΛΟΓΙΑ/ΘΠΙΣ/0308(BE)/06). The authors are grateful to M. Zamfir for useful discussions, C. S. Patrickios and E. Leontidis for providing access to the DSC apparatus and the fluorescence spectrophotometer respectively. Finally, the authors thank the A. G. Leventis Foundation for a generous donation that enabled the purchase of the NMR spectrometer from the University of Cyprus.

REFERENCES AND NOTES

1 Kim, H. N.; Guo, Z.; Zhu, H.; Juyoung, Y.; He, T. Chem Soc Rev 2011, 40, 79–93.

2 Basabe-Desmonts, L.; Reinhoudt, D. N.; Crego-Calama, M. Chem Soc Rev 2007, 36, 993–1017.

3 Ambade, A. V.; Sandanaraj, B. S.; Klaikherd, A.; Thayumanavan, S. Polym Int 2007, 56, 474–481.

4 Feng, X.; Liu, L.; Wang, S.; Zhu, D. Chem Soc Rev 2010, 39, 2411–2419.

5 Ghoroghchian, P. P.; Therien, M. J.; Hammer, D. A. Wiley Interdiscip Rev Nanomed Nanobiotechnol 2009, 1, 156–167.

6 Kalinowski, J. Opt Mater 2008, 30, 792–799.

7 Miao, L.; Liu, X.; Fan, Q.; Huang, W. Prog Chem 2010, 22, 2338–2352.

8 Hargreaves, J. S.; Webber, S. E. Macromolecules 1984, 17, 235–240.

9 Gonzalez, C.; Lim, E. C. Chem Phys Lett 2000, 322, 382–388.

10 Martínez-Máñez, R.; Sancenón, F. Chem Rev 2003, 103, 4419–4476.

11 Buruiana, E. C.; Olaru, M.; Simionescu, B. C. Eur Polym J 2007, 43, 1359–1371.

12 Hideharu, M.; Izumi, T.; Hiromi, T. Macromolecules 2010, 43, 7011–7020.

13 Shuqiang, Y.; Lei X. Hongbo, W.; Ping L. Tetrahedron 2007, 63, 7809–7815.

14 Jong-Hwa, P.; Dae, S. C.; Dong Hoon, L.; Hoyoul, K.; In Hwan, J.; Moo-Jin, P.; Nam Sung, C.; Chan Eon, P.; Hong-Ku, S. Chem Commun 2010, 46, 1863–1865.

15 Roberts, G. G.; McGinnity, M.; Barlow, W. A.; Vincett, P. S. Solid State Commun 1979, 32, 683–686.

16 Hriz, K.; Jaballah, N.; Chemli, M.; Fave, J. L.; Majdoub, M. J Appl Polym Sci 2010, 119, 1443–1449.

17 Li, T.; Chen, J.; Mitsuishi, M.; Tokuji, M. J Mater Chem 2003, 13, 1565–1569.

18 Chae, K. H.; Kim, Y. W.; Kim, T. H. Bull Korean Chem Soc 2002, 23, 1351–1354.

19 Xiaoping, Z.; Shuna, S.; Deqing, Z.; Huimin, M.; Daoben, Z. Anal Chim Acta 2006, 575, 62–67.

20 Vinyard, J. D.; Su, S.; Richter, M. M. J Phys Chem A 2008, 112, 8529–8533.

21 Baumes, M. J.; Gassensmith, J. J.; Giblin, J.; Lee, J.-J.; White, G. A.; Culligan, J. W.; Leevy, W. M.; Kuno, M.; Smith, D. B. Nat Chem 2010, 2, 1025–1030.

22 Tong, J.-D.; Zhou, C.; Ni, S.; Winnik, M. A. Macromolecules 2001, 34, 696–705.

23 Lu, J.-M.; Xu, Q.-F.; Yuan, X.; Xia, X.-W.; Wang, L.-H. J Polym Sci Part A: Polym Chem 2007, 45, 3894–3901.

24 Krasia, T.; Soula, R.; Börner, H.; Schlaad, H. Chem Commun 2003, 4, 538–539.

25 De Silva, A. P.; Gunaratne, H. Q. N.; Gunnlaugsson, T. Chem Rev 1997, 97, 1515–1566.

26 Czarnik, A. W. In Topics in Fluorescence Spectroscopy: Probe Design and Chemical Sensing; Lakowicz, J. R., Ed.; Plenum Press: New York, 1994; Vol. 4.

27 Fabbrizzi, L.; Licchelli, M.; Pallavicini, P.; Perotti, A.; Sacchi, D. Angew Chem Int Ed 1994, 33, 1975–1977.

28 Prodi, L.; Bolletta, F.; Montalti, M.; Zaccheroni, N. Coord Chem Rev 2000, 205, 59–83.

29 Corradini, R.; Paganuzzi, C.; Marchelli, R.; Pagliari, S.; Dossena, A.; Duchateau, A. J. Incl Phenom Macrocycl Chem 2007, 57, 625–630.

30 Chang, J. H.; Jeong, Y.; Shin, Y.-K. Bull Korean Chem Soc 2003, 24, 119–122.

31 Clark, M. A.; Duffy, K.; Tibrewala, J.; Lippard, S. J. Org Lett 2003, 5, 2051–2054.

32 Yanga, C.; Lee, T. S. Mol Cryst Liq Cryst 2000, 349, 283–286.

33 Chen, Z.; Xue, C.; Shi, W.; Luo, F.-T.; Green, S.; Chen, J.; Liu, H. Anal Chem 2004, 76, 6513–6518.

34 Wang, H.-W.; Cheng, Y.-J.; Chen, C.-H.; Lim, T.-S.; Fann, W.; Lin, C.-L.; Chang, Y.-P; Lin, K.-C.; Luh, T.-Y. Macromolecules 2007, 40, 2666–2671.

35 Thomas, S. W.; IIIJoly, G. D.; Swager, T. M. Chem Rev 2007, 107, 1339–1386.

36 Mehrotra, R. C.; Bohra, B.; Gaur, D. P. Metal β-Diketonates and Allied Derivatives; Academic Press:New York, 1978.

37 Teyssié, P.; Smets, G. Makromol Chem 1958, 26, 245–251.

38 Masuda, S.; Sertova, N.; Petkov, I. J Polym Sci Part A: Polym Chem 1997, 35, 3683–3688.

39 Inn, M.; Gérardin, C.; Lambard, J.; Sanchez, C. J. Sol-Gel Sci Technol 1995, 5, 101–114.

40 Masuda, S.; Minagawa, K. Prog Polym Sci 1996, 21, 557–591.

41 Agarwal, R.; Bell, J. S. Polym Eng Sci 1998, 38, 299–310.

42 Schlaad, H.; Krasia, T.; Patrickios, C. S. Macromolecules 2002, 34, 7585–7588.

43 Boyer, C.; Stenzel, M. H.; Davis, T. P. J Polym Sci Part A: Polym Chem 2011, 49, 551–595.

44 Pascual, S.; Blin, T.; Saikia, P. J.; Thomas, M.; Gosselin, P.; Fontaine, L. J Polym Sci Part A: Polym Chem 2010, 48, 5053–5062.

45 McCormick, C. L.; Lowe, A. B. Acc Chem Res 2004, 37, 312–325.

46 Venkataraman, S.; Wooley, K. L. J Polym Sci Part A: Polym Chem 2007, 45, 5420–5430.

47 Gemici, H.; Legge T. M.; Whittaker, M.; Monteiro, M. J.; Perrier, S. J Polym Sci Part A: Polym Chem 2007, 45, 2334–2340.

48 Liu, L.; Zhang, J.; Lv, W.; Luo Y.; Wang, X. J Polym Sci Part A: Polym Chem 2010, 48, 3350–3361.

49 Barner-Kowollik, C.; Davis, T. P.; Stenzel, M. H. Aust J Chem 2006, 59, 719–727.

50 Audouin, F.; Knoop, R. J. I.; Huang, J.; Heise, A. J Polym Sci Part A: Polym Chem 2010, 48, 4602–4610.

51 Kakwere, H.; Perrier, S. J Polym Sci Part A: Polym Chem 2009, 47, 6396–6408.

52 Zhu, J.-L.; Zhang, X.-Z.; Cheng, H.; Li, Y.-Y.; Cheng, S.-X.; Zhuo, R.-X. J Polym Sci Part A: Polym Chem 2007, 45, 5354–5364.

53 Luzon, M.; Boyer, C.; Peinado, C.; Corrales, T.; Whittaker, M.; Tao, L.; Davis, T. P. J Polym Sci Part A: Polym Chem 2010, 48, 2783–2792.

54 Liu, B. L.; Kazlauciunas, A.; Guthrie, J. T.; Perrier, S. Polymer 2005, 46, 6293–6299.

55 Carter, S.; Hunt, B.; Rimmer, S. Macromolecules 2005, 38, 4595–4603.

56 Carter, S.; Rimmer, S.; Sturdy, A.; Webb, M. Macromol Biosci 2005, 5, 373–378.

57 Krasia, T. C.; Patrickios, C. S. Macromolecules 2006, 39, 2467–2473.

58 Achilleos, M.; Krasia-Christoforou, T.; Patrickios, C. S. Macromolecules 2007, 40, 5575–5581.

59 Goh, Y. K.; Whittaker, A. K.; Monteiro, M. J. J Polym Sci Part A: Polym Chem 2007, 45, 4150–4153.

60 Matyjaszewski, K. Curr Opin Solid State Mater Sci 1996, 1, 769–776.

61 Moad, G.; Rizzardo, E.; Thang, S. H. Aust J Chem 2005, 58, 379–410.

62 Convertine, A. J.; Lokitz, B. S.; Lowe, A. B.; Scales, C. W.; Myrick, L. J.; McCormick, C. L. Macromol Rapid Commun 2005, 26, 791–795.

63 Moad, G.; Mayadunne, R. T. A.; Rizzardo, E. Macromol Symp 2003, 192, 1–12.

64 Buzin, A. I.; Pyda, M.; Costanzo, P.; Matyjaszewski, K.; Wunderlich, B. Polymer 2002, 43, 5563–5569.

65 Allcock, H. R.; Lampe, F. W.; Mark, J. E. Contemporary Polymer Chemistry, 3rd ed.; Pearson Education, Inc.: New Jersey, 2003.

66 Kim, J.-M.; Chang, T.-E.; Han, D. K.; Ahn, K.-D. J Photopolym. Sci. Technol 2000, 13, 273–276.

67 Krasia, T.; Schlaad, H. ACS Symp Ser 2006, 928, 157–167.

68 Weizman, H.; Ardon, O.; Mester, B.; Libman, J.; Oren Dwir, O.; Hadar, Y.; Chen, Y.; Shanzer, A. J Am Chem Soc 1996, 118, 12368–12375.

69 Wang, B.; Wasielewski, M. R. J Am Chem Soc 1997, 119, 12–21.

70 Le, T. P. T.; Moad, G.; Rizzardo, E.; Thang, S. H. PCT Int. Appl. WO 9801478 A1 980115, 1998.